

Published in final edited form as:

J Control Release. 2009 March 4; 134(2): 81–90. doi:10.1016/j.jconrel.2008.10.021.

Growth Factor Gradients via Microsphere Delivery in Biopolymer Scaffolds for Osteochondral Tissue Engineering

Xiaoqin Wang¹, Esther Wenk², Xiaohui Zhang¹, Lorenz Meinel^{1,2}, Gordana Vunjak-Novakovic³, and David L. Kaplan^{1,*}

¹ Department of Biomedical Engineering, Tufts University, 4 Colby Street, Medford, MA 02155, USA ² Institute of Pharmaceutical Sciences, Drug Formulation and Delivery Group, Swiss Federal Institute of Technology Zurich (ETH Zurich), Zurich, Switzerland ³ Department of Biomedical Engineering, Columbia University, New York, NY 10027, USA

Abstract

Temporally and spatially controlled delivery of growth factors in polymeric scaffolds is crucial for engineering composite tissue structures, such as osteochondral constructs. In the present study, microsphere-mediated growth factor delivery in polymer scaffolds and its impact on osteochondral differentiation of human bone marrow-derived mesenchymal stem cells (hMSCs) was evaluated. Two growth factors, bone morphogenetic protein 2 (rhBMP-2) and insulin-like growth factor I (rhIGF-I), were incorporated as a single concentration gradient or reverse gradient combining two factors in the scaffolds. To assess the gradient making system and the delivery efficiency of polylactic-co-glycolic acid (PLGA) and silk fibroin microspheres, initially an alginate gel was fabricated into a cylinder shape with microspheres incorporated as gradients. Compared to PLGA microspheres, silk microspheres were more efficient in delivering rhBMP-2, probably due to sustained release of the growth factor, while less efficient in delivering rhIGF-I, likely due to loading efficiency. The growth factor gradients formed were shallow, inducing non-gradient trends in hMSC osteochondral differentiation. Aqueous-derived silk porous scaffolds were used to incorporate silk microspheres using the same gradient process. Both growth factors formed deep and linear concentration gradients in the scaffold, as shown by enzyme-linked immunosorbent assay (ELISA). After seeding with hMSCs and culturing for 5 weeks in a medium containing osteogenic and chondrogenic components, hMSCs exhibited osteogenic and chondrogenic differentiation along the concentration gradients of rhBMP-2 in the single gradient of rhBMP-2 and reverse gradient of rhBMP-2/rhIGF-I, but not the rhIGF-I gradient system, confirming that silk microspheres were more efficient in delivering rhBMP-2 than rhIGF-I for hMSCs osteochondrogenesis. This novel silk microsphere/scaffold system offers a new option for the delivery of multiple growth factors with spatial control in a 3D culture environment for both understanding natural tissue growth process and *in vitro* engineering complex tissue constructs.

Keywords

silk; fibroin; alginate; polylactic-co-glycolic acid; rhBMP-2; rhIGF-I; gradient; scaffold

*Corresponding author. Phone: 617-627-3251; Fax: 617-627-3231; Email: E-mail: david.kaplan@tufts.edu.

Publisher's Disclaimer: This is a PDF file of an unedited manuscript that has been accepted for publication. As a service to our customers we are providing this early version of the manuscript. The manuscript will undergo copyediting, typesetting, and review of the resulting proof before it is published in its final citable form. Please note that during the production process errors may be discovered which could affect the content, and all legal disclaimers that apply to the journal pertain.

Introduction

Growth factors are polypeptides that can either stimulate or inhibit cellular proliferation, differentiation, migration, adhesion, and gene expression. Growth factor effects are concentration-dependent, often in a complex non-monotonic way [1]. Due to their control of many biological processes, growth factors are finding wide-spread use in the regeneration of many tissue types, such as musculoskeletal, neural, hepatic, and vascular systems [1,2]. Typically, recombinant types of growth factors are delivered in the culture medium to regulate cellular processes in the field of tissue engineering. For clinical therapies, these factors are administered either systemically or via direct injection into the tissue site of interest. However, the short half-lives, relatively large size, slow tissue penetration, and potential toxicity at the systemic level have hindered many applications for these bioactive compounds [3].

One option to enhance the *in vitro* and *in vivo* efficacy of growth factors is to incorporate them into polymeric biomaterials in order to maintain their stability and control their release kinetics. Growth factors can be incorporated directly into a polymeric scaffold to be used for tissue formation either during or after scaffold fabrication [4–6]. The release of these factors is then controlled by diffusion and/or scaffold erosion or degradation mechanisms. Growth factor delivery can also be accomplished in the form of microparticles, nanoparticles or related material formats incorporated into the scaffold [7,8,9], or via growth factor-secreting natural or genetically engineered cells harbored within the scaffolds [10,11].

One important application for growth factor delivery is in bone and cartilage tissue engineering. Degenerative diseases such as osteoarthritis, and traumatic injuries, are both prominent causes of cartilage defects. Due to the avascular nature, adult human cartilage has a limited capacity for regeneration. Therapies such as osteochondral grafting, chondroplasty, and prosthetic joint replacement have found only partial or temporary success due to inadequate donor tissue availability, donor site morbidity, the risk of infection, abrasion of the cartilage surface, loosening of implants, and limited durability of prosthetics [12]. Tissue engineering provides a promising alternative therapy, such as through engineering an osteochondral tissue that has the same structural and mechanical properties as a native cartilage-bone plug for subsequent implantation *in vivo*.

However, the fabrication of such a scaffold to control the formation of a composite bone and cartilage architecture remains a significant challenge. Since human mesenchymal stem cells (hMSCs) can differentiate into multiple tissue-forming cell lineages, such as osteoblasts, chondrocytes, adipocytes, tenocytes, and myocytes, under the stimulation of growth factors, a useful strategy is to immobilize specific growth factors in the scaffold such that the hMSCs are guided toward different tissue types with spatial control or patterning [13,14]. To date, the most commonly used strategy to engineer osteochondral construct is to fabricate a polymer scaffold consisting of two layers of materials with distinct properties, such as porosity, mechanical strength and material microstructure to mimic the natural ECM environment for bone and cartilage development. The scaffolds seeded with either hMSCs or pre-differentiated chondrocytes and osteoblasts can then be used for *in vitro* or *in vivo* studies [15–18]. Growth factors were added to the medium if the constructs were cultured *in vitro*. In some studies, growth factors have been incorporated into polymer scaffolds and the sustained release of growth factors facilitated bone and cartilage regeneration *in vitro* and *in vivo* [4–9,19–21]. However, the dose and spatial distribution of growth factors in these scaffold systems was not controlled.

It has been widely reported in the literature that bone morphogenetic protein 2 (BMP-2) and insulin-like growth factor (IGF-I) can induce hMSC osteogenic and chondrogenic differentiation, although the role of rhIGF-I in chondrogenesis still remains controversial [4,

6,8,10,20–30]. In the present study, rhBMP-2 and rhIGF-I were microencapsulated in PLGA and silk microsphere systems which were further incorporated as a single or reverse gradient in a biopolymer scaffold comprising of either alginate or silk fibroin. With different combinations of growth factors in different carrier systems, we expected to induce hMSC osteogenic and chondrogenic differentiation in one scaffold matrix with spatial control of growth factors distribution and temporal control of their release. The finding will be useful for the future fabrication of osteochondral constructs for bone repair applications. For the polymer scaffold system incorporating microspheres and supporting tissue formation, alginate gel was used for the initial scoping studies due to its long history of use for cell encapsulation [31–33], and the ease with which gels can be formed to generate microsphere/growth factor gradients. Silk porous sponge-like scaffolds were used due to their excellent biocompatible, biodegradable, and mechanical properties for tissue engineering applications [34–40]. For the microsphere systems carrying growth factors, PLGA microspheres were selected as they have been used for encapsulating growth factors, including rhBMP-2 and rhIGF-I [41–43]. Recently, silk fibroin protein was also formed into microspheres using a novel method suitable for protein encapsulation and controlled release [44]. In the present study, in parallel with PLGA microspheres, silk microspheres were also used to encapsulate rhBMP-2 and rhIGF-I. The loading and release of growth factors from the two microsphere systems, as well as the impacts of growth factor release on hMSC differentiation in different scaffold matrices were compared.

2. Materials and Methods

2.1. Materials

Cocoons of *B. mori* silkworm silk were kindly supplied by M. Tsukada (Institute of Sericulture, Tsukuba, Japan). 1,2-Dioleoyl-*sn*-glycero-3-phosphocholine (DOPC) were purchased from Avanti Polar Lipids (Alabaster, AL). rhBMP-2 was supplied by Medtronic Inc (Minneapolis, MN) and recombinant human insulin like growth factor 1 (rhIGF-I) by Tercica (Brisbane, CA). Pysigel® (80 mg/ml of succinylated gelatin) was from Braun Medical (Emmenbrucke, Switzerland). 3,3',5,5' Tetramethylbenzidine (TMB) solution was purchased from BioFX laboratories (Owing Mills, MD). Horseradish peroxidase (type VI-A), low viscosity alginate, 1,1,1,3,3,3-Hexafluoro-2-propanol (HFIP) and other chemicals were from Sigma-Aldrich (St. Louis, MO).

2.2. Purification of silk fibroin

Silk fibroin aqueous stock solutions were prepared as previously described [45]. The final concentration of silk fibroin aqueous solution was approximately 8% (w/v).

2.3. Silk microspheres encapsulating HRP, rhBMP-2 and rhIGF-I

Two hundred mg of DOPC was dissolved in 1 ml chloroform in a glass tube and dried into a film under a flow of nitrogen gas. One ml of 8% (w/v) silk fibroin solution was mixed with (1) 125 μ l of 2 mg/ml HRP, rhBMP-2 or rhIGF-I (3.125 μ g growth factor per milligram silk) in the alginate gel scaffold experiment; (2) 125 μ l of 2 mg/ml rhBMP-2 and 375 μ l of 2 mg/ml rhIGF-I (9.375 μ g growth factor per milligram silk) in the silk scaffold experiment. The mixture was added to hydrate the lipid film. The mixture of DOPC, silk and rhBMP-2 was diluted to 4 ml with water and moved to a plastic tube. The sample was frozen in liquid nitrogen for 15 min and then thawed at 37°C for 15 min. The freeze-thaw step helped form smaller vesicles with homogeneous size distributions as well as increased the protein loading [44]. This freeze-thaw cycle was repeated 3 times and then the thawed solution was slowly pipetted into a glass beaker containing 50 ml water with fast stirring. The resulting solution was lyophilized for 3 days and stored at 4°C. To prepare silk microspheres, the lyophilized material was suspended in 40 ml of pure methanol (MeOH) in a 50 ml plastic tube and the suspension was incubated for 15 min at room temperature followed by centrifugation at 9,000 rpm for 20 min

at 4°C (Sorvall RC-5B centrifuge). MeOH was used in this case to remove the lipid templates and induce silk self-assembly (β -sheet structure) to form silk microspheres with an average diameter of about 1.6 μm [44]. The pellet obtained was dried in air and stored at 4°C before use (Supplemental Figure A)

2.4. PLGA microspheres encapsulating HRP, rhBMP-2 and rhIGF-I

PLGA microspheres were prepared by solvent evaporation from a water-in-oil-in-water ($W_1/O/W_2$) dispersion [46]. Details are provided in the Supplemental Materials.

2.5. Determination of loading and release of rhBMP-2 and rhIGF-I from silk microspheres

Silk microspheres loaded with rhBMP-2 or rhIGF-I (initial loading of 3.125 $\mu\text{g}/\text{mg}$ silk for both) were suspended in phosphate buffer, pH 7.2 to a concentration of 20 mg/ml of microspheres. The microspheres were dispersed by ultrasonication. One ml of suspension (20 mg/ml) was used for growth factor loading and release study. To determine loading, 1 ml of suspension was lyophilized and the dried material was treated with hexafluoroisopropanol (HFIP), and dissolved in 1 ml phosphate buffer at pH 7.2. rhBMP-2 or rhIGF-I content was determined using an BMP-2 or IGF-I ELISA kit (R&D systems, Minneapolis, MN). To determine rhBMP-2 or rhIGF-I release, a 1 ml silk microsphere suspension was incubated at 37°C. At desired time points, the suspensions were centrifuged at 10,000 rpm for 2 min. The supernatant was moved to another tube and the pellet was resuspended in 1 ml fresh buffer. rhBMP-2 or rhIGF-I content in the supernatant was determined by ELISA. The actual loading was then obtained by comparing growth factor content with the initial loading (3.125 $\mu\text{g}/\text{mg}$ silk), and the percentage of release was obtained by comparing with loading. All experiments were performed in triplicate.

2.6. Culture of human bone marrow-derived mesenchymal stem cells (hMSCs)

hMSCs were isolated from fresh whole bone marrow aspirates from consenting donors (Clonetic-Poietics, Walkersville, MD) as described previously [47]. Passage 3–4 cells were used for encapsulation studies. All cell cultures were maintained at 37°C in an incubator with 95% air and 5% CO_2 . The cultures were replenished with fresh medium at 37 °C twice a week.

2.7. Gradient incorporation of PLGA or silk microspheres and hMSCs in an alginate gel scaffold

PLGA and silk microspheres loaded with either rhBMP-2 or rhIGF-I were suspended in 2.5 % (w/v) alginate solution to a concentration of 20 mg/ml. The clustered microspheres were dispersed by ultrasonication for 10 sec at 30% amplitude (approximately 20 W) using a Branson 450 ultrasonicator (Branson Ultrasonics Co., Danbury, CN). hMSCs were trypsinized and suspended with 2.5 % (w/v) alginate solution containing or not containing microspheres to a final density of 1.5×10^6 cells/ml. The suspensions were used immediately to make gel scaffolds using a modified gradient maker with two connected chambers (CBS Scientific, Temecula CA). To obtain a linear concentration gradient, the two chambers should contain two solutions of equal volume (minimal volume of 0.5 ml), each of which contained a different concentration of silk microspheres but the same concentration of hMSCs. The center valve was closed prior to mixing. Alginate sodium salt was dissolved in distilled water to a final concentration of 2.5% (w/v) and sterilized by filtration through a 0.22 μm membrane. To prepare rhBMP-2 gradient gels, 0.5 ml of 2.5 % (w/v) alginate solution containing hMSCs (1.5×10^6 cells/ml) was added to chamber A, and 0.5 ml of 2.5% (w/v) alginate solution containing 6 mg rhBMP-2-silk microspheres and hMSCs was added to chamber B. The stir bar in chamber B was then activated, the center valve opened, and the peristaltic pump started. As the solution in chamber A was drawn through the conduit it mixed completely with the solution in chamber B, and the volumes of chamber A and B were simultaneously depleted. A linear rhBMP-2-silk

microsphere gradient was formed because the 0 mg/ml microsphere suspension in chamber A was mixed with an increasingly lower volume of microsphere suspension in chamber B. The mixed solution was eluted through a glass pipette (diameter = 2 mm) into a glass tube containing 25 mM CaCl₂ solution. The glass pipette was positioned at the bottom of the tube at the beginning, and it was lifted slowly while the solution was eluted to allow the gel to form and to keep the cylindrical shape in the tube. The gel scaffolds formed were approximately 10 cm in length and 2–3 mm in diameter. After incubation for about 10 min in the CaCl₂ solution, the completely formed gel scaffold was washed with PBS and moved to a 6-well plate containing 4 ml of growth medium. To prepare rhIGF-I gradient scaffolds, rhIGF-I encapsulated PLGA or silk microspheres were used in chamber B and the rest of the system was the same as described above. To prepare a control scaffold, empty PLGA or silk microspheres were used in chamber B and the rest was the same as above. To prepare rhIGF-I/rhBMP-2 reverse gradient scaffolds, rhIGF-I encapsulated PLGA or silk microspheres were used in chamber A and rhBMP-2 encapsulated microspheres were used in chamber B, and the rest was the same as described above.

2.8. HRP gradient determination in alginate scaffolds

HRP-encapsulated PLGA or silk microspheres were incorporated in alginate gel scaffolds as described above (please see Supplemental Materials for details).

2.9. Gradient incorporation of silk microspheres in a silk porous 3D scaffold

Silk scaffolds with gradients of rhBMP-2 and rhIGF-I were obtained using the same experimental set up but 0.5 ml 6% (w/v) silk solution with or without 20 mg of silk microspheres. The mixed solution from the gradient maker was eluted through a needle into a glass mold (inner diameter = 10 mm; height = 30 mm). Sieved sodium chloride particles with sizes between 500 to 600 μm were slowly added to the glass mold with a speed matching the eluting silk solution. Three different scaffolds, rhBMP-2 gradients, rhIGF-I gradients and rhBMP-2/rhIGF-I inverse gradients, as well as the control scaffold containing empty microspheres were prepared. The glass molds were covered and stored at room temperature for 24 hours to permit the silk to undergo a structural transition to a beta sheet, forming physical crosslinks to stabilize the 3D matrix as we have previously reported [37]. To leach out the NaCl particles and obtain the porous scaffold, the glass molds were immersed in 1 liter of ultrapure (MilliQ) water with stirring, and the scaffold was removed from the mold after about 30 min and washed for 8 hours by changing the water three times. Each scaffold was cut into 4 parts along the gradient direction, and the small scaffolds (length ≈ 2.5 cm; diameter ≈ 2 mm) were immediately used for cell culture or lyophilized and used for SEM and ELISA analysis.

2.10. Enzyme-linked immunosorbent assay (ELISA)

rhBMP-2 and rhIGF-I content in the 3D porous silk scaffolds was quantified by ELISA (kit from R&D systems, Minneapolis, MN). Briefly, a 30 mm long scaffold after salt leaching was cut into 7 pieces along the long axis, and each piece was placed in an Eppendorf tube and lyophilized. The dried material was suspended in 250 μl of HFIP which functioned to solubilize the silk and release the contained growth factors [45]. The tube was closed and incubated overnight at room temperature. HFIP was then evaporated by a flow of nitrogen gas and the dried protein was dissolved in 1 ml phosphate buffer, pH 7.2. rhIGF-I content in the solution was detected by ELISA. The solution was diluted 5, 50, and 500 fold with the same buffer, and the three solutions, as well as the diluted standards for rhBMP-2 and rhIGF-I, were subjected to ELISA following the supplier's instructions. All experiments were performed in triplicate.

2.11. hMSC seeding and culture in alginate and silk scaffolds

For the alginate gel scaffolds, hMSCs were encapsulated in the gel during gel formation as described above. After preparation, the scaffolds were cultured in growth medium overnight and then moved and cultured in the osteochondral medium containing 90% DMEM, 10% fetal bovine serum (FBS), 0.1 mM non-essential amino acids, ITS⁺ (10 µg/ml insulin, 5.5 µg/ml transferrin, 5 ng/ml selenium, 0.5 mg/ml bovine serum albumin, 4.7 µg/ml linoleic acid, Sigma), 50 µg/ml ascorbic acid, 10 nM dexamethasone, 10 mM β-glycerolphosphate, 100 U/mL penicillin, 1000 U/mL streptomycin, and 0.2% fungizone antimycoticin for 3 weeks. The medium was replenished twice a week. After culture, each scaffold was washed with PBS, cut into 11 segments along the long axis, and either immersed in 10% neutral buffered formalin for histology, immediately subjected to RNA extraction, or stored at -80°C for calcium assay. For the 3D porous silk, the scaffolds were immersed in 2 ml of 70% ethanol for 30 min in a 12-well plate for sterilization, and this process was repeated three times. The scaffolds were then washed three times with phosphate buffer at pH 7.2 followed by incubation in 2 ml of growth medium at 37°C overnight. Before use, the medium was aspirated from the scaffolds, and hMSCs suspension (5×10^6 in 100 µL growth medium) was evenly seeded onto each scaffold. The constructs were kept in a 37°C incubator for 2 h to allow the cells to diffuse into and attach to the scaffolds before 2mL of fresh medium was added. One milliliter DMEM was added in empty wells in the seeding plates to maintain moisture. Twenty-four hours later, each construct was transferred to a blank well in a different plate and replenished with osteochondral medium as mentioned earlier. The constructs were cultured at 37°C for 5 weeks by the replenishment of fresh medium twice a week. After culture, each construct was washed with PBS, cut into 7 segments along the long axis, and immersed in 10% neutral buffered formalin for histology, immediately subjected to RNA extraction, or stored at -80°C for calcium assay. At least 3 scaffolds were used in each group.

2.12. Phase contrast and Scanning electron microscopy (SEM)

The alginate scaffolds with encapsulated hMSCs and microspheres were transparent enough for microscopic imaging during culture. A phase contrast light and fluorescence microscope (Carl Zeiss, Jena, Germany) equipped with a Sony Exwave HAD 3CCD color video camera was used. SEM was used to determine the distribution of silk microspheres in the silk scaffolds and the tissue formation at the end of culture. Various silk scaffolds were washed with phosphate buffer at pH 7.2 and lyophilized for 3 days, quickly frozen in liquid nitrogen, and cross-sectioned into thin pieces with a razor. The pieces of scaffold were fixed on sample mounts, sputter-coated with Au using a Ploaron SC502 Sputter Coater (Fison Instruments, UK), and examined using a JEOL JSM 840 Scanning Electron Microscope (Peabody, MA) at 15 KV.

2.13. Total RNA extraction, cDNA synthesis, and real-time RT-PCR analysis

Total RNA was extracted from cells using an RNeasy Mini Kit (Qiagen, Valencia, CA, USA) following the supplier's instructions. Please see Supplemental Materials for additional details.

2.14. Calcium and glycosaminoglycans (GAG) assay

After culture, the constructs were cut into small segments which were quickly dried on tissue paper and weighed. For calcium determination, samples were then extracted with 0.5 ml of 5% trichloroacetic acid for 30 min at room temperature, centrifuged at 12,000 rpm for 5 min at room temperature (Eppendorf 5417R centrifuge), and the calcium content in the supernatant was determined spectrophotometrically at 575 nm, following reaction with o-cresolphthalein complexone according to the manufacturer's instructions (Sigma). The calcium content was normalized by sample wet weight (% w/w). For GAG determination, samples were digested in 0.14 mg/ml papainase in a buffer containing 100 mM phosphate, 10 mM

ethylenediaminetetraacetate (EDTA), and 10 mM cysteine for 15 h at 60°C. GAG content was determined spectrophotometrically at 656 nm following reaction with dimethylmethylene blue dye, according to the manufacturer's protocol (Blyscan™, Biocolor Ltd., Newtownabbey, Northern Ireland). All experiments were performed in triplicate.

2.15. Histology and immunohistochemistry

Scaffolds seeded with cells were washed in PBS and fixed in 10% neutral buffered formalin for 2 days before histological analysis. Samples were dehydrated through a series of graded ethanol, embedded in paraffin and sectioned at 5 mm thickness. For histological evaluation, sections were deparaffinized, rehydrated through a series of graded ethanols, and stained with hematoxylin and Eosin (H&E), Alcian blue (pH 2.5) and von Kossa with a fast red counterstaining. For immunohistochemical evaluation, sections were incubated with a mouse anti-human Col-I antibody and a mouse anti-human Col-II antibody (Chemicon, Temecula, CA) before the horseradish peroxidase (HRP)-labeled secondary antibody and processed with a BenchMark-automated histology staining system (Ventana, Tucson, AZ). Sections were counterstained with hematoxylin.

2.16. Statistics

All experiments were performed with a minimum of $N = 3$ for each data point. Statistical analysis was performed by one-way analysis of variance (ANOVA) and Student-Newman-Keuls Multiple Comparisons Test. Differences were considered significant when $p \leq 0.05$, very significant when $p \leq 0.01$, and extremely significant when $p \leq 0.001$.

3. Results

3.1. Gradient delivery study using alginate gel scaffolds

3.1.1. PLGA and silk microsphere preparation and sustained growth factor release—Growth factors, i.e., rhBMP-2 and rhIGF-I, and a model protein drug, horseradish peroxidase (HRP), were encapsulated in either PLGA or silk microspheres (Supplemental Figure A). The loading of rhBMP-2 and rhIGF-I in silk microspheres was 0.3 and 0.45 $\mu\text{g}/\text{mg}$ silk microspheres, respectively, corresponding to 41% and 14% loading efficiency (Supplemental Table 1). The cumulative release profiles of the two growth factors were different. rhIGF-I showed a burst release with approximately 40% of total rhIGF-I released in the first 2 days. The release then decreased, with approximately 70% of total rhIGF-I released after 14 days (Supplemental Figure B). rhBMP-2, however, showed almost no burst release, and the overall release was slow and sustained. Less than 15% of total rhBMP-2 was released within 14 days. This is similar to the release of horseradish peroxidase (HRP) from silk microsphere in our previous studies [44].

3.1.2. Gradient incorporation of microspheres in alginate scaffolds—PLGA or silk microspheres encapsulating HRP were incorporated in a cylinder-shaped alginate gel scaffold using a gradient gel maker as shown in Figure 1B. The HRP concentration in the scaffold was determined by sectioning of the scaffold along its longitudinal direction and measuring enzyme activity in each fragment. When alginate concentration of 2.5% (w/v) was used, linear gradient distribution of HRP was observed in both PLGA and silk microsphere-incorporated scaffolds (Figure 1A,B). The gradient was shallow (approximately 2-fold increase of HRP content through the scaffold), with relatively low R^2 (0.75) after fitting the data with least-squares linear regression (Figure 1A,B). Scaffolds prepared at lower alginate concentration (1.2% (w/v)) did not show satisfying HRP gradients, especially for PLGA-microsphere incorporation (data not shown).

3.1.3. hMSCs encapsulation and differentiation in alginate scaffolds—hMSCs at passage 3 were trypsinized and mixed with alginate/microsphere suspension. The mixture was used to prepare cylinder-shaped gels as described above. Under microscope, the gels were opaque when silk microspheres (about 6 mg) were incorporated, while transparent when the same amount of PLGA microspheres were incorporated (Figure 1C). The PLGA microspheres and hMSCs were distinguishable and appeared uniformly distributed in the gels (Figure 1C). hMSCs remained rounded throughout the culture period, similar to the control sample of hMSCs encapsulated in the alginate gel in the absence of microspheres (data not shown).

In response to the release of growth factors from microspheres, hMSCs conducted osteogenic and chondrogenic differentiation during 3 weeks culture time and the levels were examined along the scaffold. Comparing PLGA and silk microsphere delivery system, the later is more efficient in delivering rhBMP-2 to induce hMSCs osteogenesis. The Col I and BSP transcript level in the single BMP-2-silk microsphere gradient and BMP-2/IGF-I-silk microsphere reverse gradient scaffold was significantly higher ($p < 0.001$) than that in the corresponding PLGA microsphere-incorporated scaffolds (Figure 2A,B,C). The rhIGF-I-PLGA microsphere system, however, induced about 10 fold increase of BSP transcript level, higher than that in the rhIGF-I-silk microsphere system, which showed almost no increase ($p < 0.001$, Figure 2B). Therefore, both rhBMP-2 and rhIGF-I induced hMSC osteogenesis, and their efficacies were dependent on the encapsulation microsphere system used. Similarly, hMSC chondrogenesis was also induced by rhBMP-2 and rhIGF-I, as determined by Col II gene expression (Figure 2D). PLGA microsphere system is more efficient than silk microsphere system in this case in delivering rhBMP-2 or rhIGF-I for chondrogenesis ($p < 0.001$, Figure 2D). Silk microspheres, however, were better than PLGA microspheres for exhibiting the reverse dual gradient of rhBMP-2 and rhIGF-I, as seen by upregulated Col II gene expression ($p < 0.001$, Figure 2D). For both PLGA and silk delivery systems, the levels of hMSC differentiation did not follow the gradient trend of rhBMP-2 and/or rhIGF-I; they were more randomly distributed in the scaffolds (Figure 2A–D). This might be due to the shallow gradient distribution of microspheres and/or the fast diffusion of released growth factors in the aqueous alginate gel environment.

3.2. Osteochondral tissue engineering using silk gradient scaffolds

3.2.1. Gradient distribution of silk microspheres and growth factors in silk scaffold—The same gradient making system as described above was used to prepare elongated silk scaffolds with silk microspheres incorporated as concentration gradients. The scaffolds were white and soft, with a diameter about 2 – 3 mm and length about 25 mm. When rhBMP-2 and rhIGF-I encapsulated silk microspheres were used, both growth factors were immobilized as concentration gradients in the scaffolds as the result of gradient incorporation of microspheres, as determined by ELISA on scaffold segments (Figure 3A,B). The growth factor gradients formed were deeper and more linear, with $R^2 = 0.92$ and 0.95 for rhBMP-2 and rhIGF-I, respectively, as compared with those in the alginate gel system. Furthermore, microspheres were evenly distributed in the scaffold with no aggregates or big clusters formed, as determined by SEM (please see Supplemental Figure C). Apparently, silk sponge-like scaffold is superior to alginate gel scaffold for incorporating microspheres and forming growth factor gradients, probably due to its unique encapsulation and diffusion-limited property based on crystalline β -sheet structure formation.

3.2.2. Gradient bone and cartilage formation in silk scaffolds—hMSCs were seeded in the silk scaffolds containing growth factor-encapsulated microspheres or empty microspheres that served as a control, and the constructs were cultured in an osteochondrogenic medium for 5 weeks. Compared to the scaffolds prior to cell seeding, the scaffolds after culture were completely filled with new extracellular matrix based on SEM imaging (Supplemental Figure C). The formation of bone and cartilage tissue in the sectioned

segments was evaluated at transcript and biochemical levels. From segment 1 to 7 (rhBMP-2 concentration increased and/or rhIGF-I concentration decreased), osteogenic markers Col I and BSP showed a corresponding increase of transcript level along the rhBMP-2 gradient (Figure 4A,B). Calcium deposition in the same segments showed a similar trend along the gradient increase (Figure 4C). Similarly, the trend along the gradient was found for hypertrophic chondrogenic marker Col X and chondrogenic marker Col II (Figure 4D,E), and GAG production (Figure 4F). For all the gene markers being tested, the transcript levels in the rhBMP-2/rhIGF-I reverse gradient scaffold were significantly higher than those in the single rhBMP-2 gradient ($p < 0.01$, Figure 4A–F). Apparently, the presence of rhIGF-I enhanced the effect of rhBMP-2 in inducing hMSC osteogenesis and chondrogenesis, a phenomenon that was not observed in alginate gel scaffold. rhIGF-I alone did not induce significant osteogenesis in the scaffold at either the transcript or biochemical level; no trend along the gradient was observed (data not shown), similar to that was observed in alginate gel scaffold. The tissue construct with the maximal outcomes (rhBMP-2/rhIGF-I inverse gradient) was subjected to histological analysis. Hematoxylin and eosin (H&E) staining revealed heterogeneous cell morphologies, e.g., osteoblast-like (cuboidal) and chondrocyte-like (spherical) cells, in the region with the highest rhBMP-2 concentration (segment 7), while most cells in the region with the lowest rhBMP-2 concentration (segment 1) retained hMSCs morphology (spindle) (Figure 5). Alcian Blue staining revealed deposition of cartilage-specific proteoglycan, forming lacunae-like ECM around chondrocyte-like cells, in segment 7. Von Kossa staining revealed bone-specific calcium deposition in the same region. Both stainings were weaker in segment 1. Therefore, the histological analysis confirmed gradient bone and cartilage formation in silk scaffold.

4. Discussion

rhBMP-2 and rhIGF-I have been encapsulated in 50:50 PLGA microspheres using W/O/W-double emulsion-solvent evaporation method, and their *in vitro* release has been characterized [26,41–43,46]. In the absence of co-encapsulated excipients, the loading efficiency of rhBMP-2 and rhIGF-I were about 50 and 23%, respectively, and the release of latter was more than 2 times faster than that of the former. Co-encapsulation with excipients largely improved loading and retarded release [43,46] (Supplemental Table 1). In our study, we used 25% Physiogel[®] as co-encapsulation excipient for rhBMP-2 and rhIGF-I encapsulation in PLGA microspheres, the same condition as used in the literature [46]. No excipient was used for silk microsphere encapsulation. The loading and loading efficiency of rhBMP-2 in silk microspheres were higher than those of rhIGF-I (Supplemental Table 1). This is similar to the results of PLGA microsphere encapsulation when no co-encapsulation excipient was used (Supplemental Table 1), suggesting that the two microsphere systems might have a similar encapsulation mechanism for rhBMP-2. It has been reported in the literature that rhBMP-2 has high binding affinity to the carboxylic acid group at the end of each PLGA polymer chain; a greater acid number of the PLGA polymer may result in a greater amount of “bound” rhBMP-2 [48]. Since there are more than 60 carboxylic acid groups in each silk fibroin molecule, rhBMP-2 might have bound to silk fibroin based on the same binding mechanism. This hypothesis, however, will need further investigation in the future studies. The release of rhBMP-2 from silk microspheres as determined in the present study is more sustained than that from PLGA microspheres as reported in the literature (Supplemental Table 1). Except for the aforementioned charge-based binding mechanism, extensive crystalline β -sheet structure network formed in silk microspheres might have also limited rhBMP-2 diffusion out of the microspheres, as we have previously reported [44].

A gradient gel maker was used to prepare alginate gel scaffolds with gradient distributions of microspheres but even distribution of hMSCs. The gel prepared had a cylindrical shape with a length about 10 cm and diameter about 2 mm. The small diameter facilitated transport of

nutrients and metabolic products through the gel. The size of microspheres and the concentration of alginate solution (related to viscosity) were found to be important in forming a good microsphere gradient. PLGA microspheres (50 – 80 μm) used in the study are much bigger than silk microspheres (< 2 μm), so that they were more rapidly precipitating in a alginate solution during the gelation in the calcium chloride solution. Silk microspheres could form linear gradient in the gel scaffold when an alginate concentration of 1.2% w/v was used, while PLGA microspheres could only form gradients at higher alginate concentrations (above 2.5% w/v). We therefore used 2.5% alginate solution for all the preparations.

To encapsulate cells, hMSCs at passage 3 were trypsinized and added to alginate solution containing or not containing microspheres to reach a cell density of 1.5×10^6 cells/ml, and the mixtures were immediately used for making gradient gel scaffold. The scaffolds prepared were then moved to a medium containing osteogenic and chondrogenic components, and cultured for 3 weeks. hMSCs remained round shape during the whole culture period. Apparently, the alginate gel environment restricted any hMSC morphology changes, a phenomenon previously reported and believed to be a prerequisite for the initiation of hMSCs differentiation process [49,50]. Further study showed that hMSCs osteogenic differentiation occurred mainly in rhBMP-2 or rhBMP-2/rhIGF-I silk microsphere gel system but very little in the corresponding PLGA microsphere gel system (Figure 2A–C). This might be due to: (1) silk microspheres released rhBMP-2 in a sustained manner and the released rhBMP-2 can reach the cells more quickly and homogeneously than that released from PLGA microspheres. (2) rhBMP-2 lost its bioactivity after being released from PLGA microspheres because of the acidic microenvironment caused by PLGA degradation. In contrast, rhIGF-I alone only induced BSP gene expression in PLGA microsphere system but not in silk microsphere system. This can be explained by different loading levels of rhIGF-I in the two microsphere systems. The loading efficiency of rhIGF-I (in the presence of 25% Physiogel[®] as co-encapsulated excipient) was about 77% in PLGA microspheres whereas it was only about 14% in silk microspheres (Supplemental Table 1). Since rhIGF-I was added in the same amount during microsphere fabrications, the rhIGF-I loading in PLGA microspheres should be more than 5 times higher than that in silk microspheres. Therefore, the amount of rhIGF-I released from silk microspheres during the culture might be below the threshold to induce hMSCs osteogenesis. For hMSC chondrogenesis, the PLGA microsphere system encapsulating rhBMP-2 or rhIGF-I was more efficient than the corresponding silk microsphere system, while the silk microsphere system was more efficient for the combination of the two growth factors (Figure 2D). All these results suggest that besides growth factors themselves, different carrier matrices that exhibit distinguished growth factor loading and release properties are also important in determining hMSC differentiation. In the alginate gel scaffold system, the level of osteochondrogenic differentiation did not follow the gradient trend of rhBMP-2 or rhIGF-I in either of the cases (Figure 2A–D). Either the gradient was too shallow or the gradient of growth factors could not be retained after release due to fast diffusion of molecules in aqueous alginate gel environment. This was improved in the following study when silk sponge porous scaffolds were used and culture time was extended to 5 weeks.

In our previous studies, water-based silk porous scaffolds were prepared by adding sodium chloride particles to silk solution to quickly induce self-assembly and gelation of silk fibroin protein [37]. After leaching out the salt, sponge-like silk scaffolds formed with the pore sizes defined by the sodium chloride particle size. The method was used in this study to prepare microsphere-gradient silk scaffold as shown in Supplemental Figure A. Only silk microspheres were used in this study. Due to fast immobilization of silk microspheres in the scaffold, suitable growth factor (rhBMP-2 and rhIGF-I) gradients could be formed along the scaffold, as determined by ELISA. After seeding hMSCs in the porous scaffold, sustained local release of growth factors effectively induced hMSC differentiation. As expected, the level of hMSC osteogenic and chondrogenic differentiation was controlled by the presence of rhBMP-2,

forming a gradient. The presence of rhIGF-I enhanced the effect of rhBMP-2 in the reverse dual gradient scaffold, a phenomenon not observed in the alginate gel scaffold. This might be due to higher retention of rhIGF-I in silk crystalline β -sheet matrix than in alginate gel matrix. The rhIGF-I alone, however, did not induce osteochondral differentiation, consistent with the alginate scaffold study. As discussed above, limited loading and relatively fast release of rhIGF-I from silk microspheres might account for the result.

The present study has demonstrated that bioactive growth factors can be delivered efficiently in a polymer scaffold via microsphere encapsulation, inducing and controlling the differentiation of seeded hMSCs. In previous studies, rhBMP-2 was added to the culture medium (1 $\mu\text{g/ml}$) to stimulate osteogenic differentiation of hMSCs that were seeded on silk 3D porous scaffolds [51]. The calcium content was approximately 2 wt% of scaffold wet weight after 5 weeks culture, similar to that formed in the rhBMP-2-incorporated scaffold and less than that in the rhBMP-2/rhIGF-I-incorporated scaffold in the present study (Figure 4C). However, the amount of rhBMP-2 used in the previous study was at least 10 times higher than that used in the present study (approximately 4 $\mu\text{g/scaffold}$). Therefore, growth factors can be delivered much more efficiently via microsphere incorporation in the scaffolds than supplemented in a soluble form in the culture medium. In two other studies, rhBMP-2 was either directly incorporated into silk scaffolds or released from genetically modified hMSCs that were seeded on silk scaffolds [25,52]. In both cases, the release of rhBMP-2 in the culture medium dropped to undetectable levels within 2–3 weeks, resulting in a lower level of calcium deposition in the scaffolds (0.4 wt% and 0.8 wt%, respectively). Furthermore, the present study showed that growth factors can be immobilized as concentration gradients in the scaffold via microsphere incorporation. Due to its aqueous gel property, alginate might not be an ideal material to retain growth factor gradients after release. Self-assembled silk material, however, is composed of extensive crystalline β -sheet structure networks which are effective physical barriers to restrict molecular diffusion [44], so that the growth factors released from microspheres could be entrapped and gradients retained in the scaffolds. Based on the present silk scaffolding system, multiple growth factors can be studied simultaneously in a 3D environment in order to screen for optimal doses and combinations. Depending on the growth factor properties, the loading and release profiles can be controlled by using various microencapsulation systems, e.g., PLGA and silk microspheres. Such growth factor delivery scaffold systems will be useful not only for understanding natural tissue growth and regeneration processes, but also for *in vitro* engineering composite tissue constructs, such as osteochondral plugs. For this, the system should further optimized by: (a) increase in the amount of growth factors incorporated in the scaffold. The highest concentration of rhBMP-2 and rhIGF-I immobilized in the silk scaffolds was about 0.45 $\mu\text{g/mg}$ dry scaffold (30 $\mu\text{g/ml}$ wet scaffold), similar to the doses used in the literature for bone and cartilage repair [26–28, 53]. This concentration, however, did not induce the highest hMSCs osteogenesis and chondrogenesis because the increase of transcript and biochemical levels did not reach plateaus (Figure 4). Either more microspheres could be incorporated in the scaffolds or the loading of growth factors in microspheres increased. (b) The release kinetics of rhBMP-2 and rhIGF-I in the silk delivery system will need to be optimized. It has been reported that sequential delivery of BMP-2 and IGF-I in a two-layered gelatin delivery system resulted in better bone formation than the simultaneous release of the two growth factors [54]. Different outcomes may be obtained if silk microspheres with distinct release properties are used in the scaffolds [44]. (c) The medium composition will need to be optimized. The osteochondrogenic medium used in the present study contained both osteogenic and chondrogenic components. Some osteogenic components, e.g., β -glycerolphosphate, may inhibit hMSC chondrogenesis.

5. Conclusions

Growth factors, rhBMP-2 and rhIGF-I, can be functionally encapsulated in either PLGA or silk microspheres and further incorporated in alginate and silk scaffolds to form concentration gradients. Depending on the nature of carrier matrices and the microencapsulation process, the two microsphere systems had distinguished growth factor loading and release properties, which impact differently on hMSC osteochondral differentiation. Silk sponge-like scaffolds were superior to alginate gel scaffolds in forming deep linear growth factor gradients. The osteogenic and chondrogenic differentiation of hMSCs seeded in these silk scaffolds corresponded to the gradient distribution of rhBMP-2 and reverse distribution of rhBMP-2/rhIGF-I, showing a trend of gradient increase. rhIGF-I enhanced the effect of rhBMP-2 but it alone did not induce hMSC differentiation, probably due to its limited loading and fast release. Therefore, control of specific tissue formation can be achieved by controlling spatial distribution of growth factors in a polymer scaffold via microsphere incorporation.

Supplementary Material

Refer to Web version on PubMed Central for supplementary material.

Acknowledgments

We thank Yongzhong Wang and Charu Vepari (Tufts University) for useful discussions throughout the project, Hyeon-Joo Kim (Tufts University) for help with histological and immunohistochemical analysis. We thank Paola DeLeon at Medtronic Inc. (Minneapolis, MN) for the rhBMP-2, and Corina Hughes-Klemm in Tercica Inc (Brisbane, CA) for the rhIGF-I. The study was supported by the NIH P41 Tissue Engineering Resource Center and the NIH NIBIB (EB003210).

References

1. Babensee JE, McIntire LV, Mikos AG. Growth factor delivery for tissue engineering. *Pharm Res* 2000;17:497–504. [PubMed: 10888299]
2. Boontheekul T, Mooney DJ. Protein-based signaling systems in tissue engineering. *Curr Opin Biotechnol* 2003;14:559–565. [PubMed: 14580589]
3. Edelman ER, Nugent MA, Karnovsky MJ. Perivascular and intravenous administration of basic fibroblast growth factor: vascular and solid organ deposition. *Proc Natl Acad Sci USA* 1993;90:1513–1517. [PubMed: 8434012]
4. Whang K, Tsai DC, Nam EK, Aitken M, Sprague SM, Patel PK, Healy KE. Ectopic bone formation via rhBMP-2 delivery from porous bioabsorbable polymer scaffolds. *J Biomed Mater Res* 1998;42:491–499. [PubMed: 9827671]
5. Uebersax L, Merkle HP, Meinel L. Insulin-like growth factor I releasing silk fibroin scaffolds induce chondrogenic differentiation of human mesenchymal stem cells. *J Control Release* 2008;127:12–21. [PubMed: 18280603]
6. Li C, Vepari C, Jin HJ, Kim HJ, Kaplan DL. Electrospun silk-BMP-2 scaffolds for bone tissue engineering. *Biomaterials* 2006;27:3115–3124. [PubMed: 16458961]
7. Hosseinkhani H, Hosseinkhani M, Khademhosseini A, Kobayashi H. Bone regeneration through controlled release of bone morphogenetic protein-2 from 3-D tissue engineered nano-scaffold. *J Control Release* 2007;117:380–386. [PubMed: 17207881]
8. Luginbuehl V, Wenk E, Koch A, Gander B, Merkle HP, Meinel L. Insulin-like growth factor I-releasing alginate-tricalciumphosphate composites for bone regeneration. *Pharm Res* 2005;22:940–950. [PubMed: 15948038]
9. Chung YI, Ahn KM, Jeon SH, Lee SY, Lee JH, Tae G. Enhanced bone regeneration with BMP-2 loaded functional nanoparticle-hydrogel complex. *J Control Release* 2007;121:91–99. [PubMed: 17604871]

10. Gelse K, von der Mark K, Aigner T, Park J, Schneider H. Articular cartilage repair by gene therapy using growth factor-producing mesenchymal cells. *Arthritis Rheum* 2003;48:430–441. [PubMed: 12571853]
11. Pagnotto MR, Wang Z, Karpie JC, Ferretti M, Xiao X, Chu CR. Adeno-associated viral gene transfer of transforming growth factor-beta1 to human mesenchymal stem cells improves cartilage repair. *Gene Ther* 2007;14:804–813. [PubMed: 17344902]
12. Grande DA, Breitbart AS, Mason J, Paulino C, Laser J, Schwartz RE. Cartilage tissue engineering: current limitations and solutions. *Clin Orthop Relat Res* 1999;367 Suppl:S176–185. [PubMed: 10546646]
13. Rahaman MN, Mao JJ. Stem cell-based composite tissue constructs for regenerative medicine. *Biotechnol Bioeng* 2005;91:261–284. [PubMed: 15929124]
14. Hench LL, Polak JM. Third-generation biomedical materials. *Science* 2002;295:1014–1017. [PubMed: 11834817]
15. Chen G, Sato T, Tanaka J, Tateishi T. Preparation of a biphasic scaffold for osteochondral tissue engineering. *Mater Sci Eng C* 2006;26:118 – 123.
16. Shao XX, Hutmacher DW, Ho ST, Goh JC, Lee EH. Evaluation of a hybrid scaffold/cell construct in repair of high-load-bearing osteochondral defects in rabbits. *Biomaterials* 2006;27:1071–1080. [PubMed: 16129483]
17. Chang CH, Lin FH, Lin CC, Chou CH, Liu HC. Cartilage tissue engineering on the surface of a novel gelatin-calcium-phosphate biphasic scaffold in a double-chamber bioreactor. *J Biomed Mater Res B Appl Biomater* 2004;71:313–321. [PubMed: 15386400]
18. Tuli R, Nandi S, Li WJ, Tuli S, Huang X, Manner PA, Laquerriere P, Noth U, Hall DJ, Tuan RS. Human mesenchymal progenitor cell-based tissue engineering of a single-unit osteochondral construct. *Tissue Eng* 2004;10:1169–1179. [PubMed: 15363173]
19. Tabata Y, Yamada K, Miyamoto S, Nagata I, Kikuchi H, Aoyama I, Tamura M, Ikada Y. Bone regeneration by basic fibroblast growth factor complexed with biodegradable hydrogels. *Biomaterials* 1998;19:807–815. [PubMed: 9663757]
20. Boyan BD, Lohmann CH, Somers A, Niederauer GG, Wozney JM, Dean DD, Carnes DL Jr, Schwartz Z. Potential of porous poly-D,L-lactide-co-glycolide particles as a carrier for recombinant human bone morphogenetic protein-2 during osteoinduction in vivo. *J Biomed Mater Res* 1999;46:51–59. [PubMed: 10357135]
21. Winn SR, Uludag H, Hollinger JO. Carrier systems for bone morphogenetic proteins. *Clin Orthop Relat Res* 1999;367 Suppl:S95–106. [PubMed: 10546639]
22. Shea CM, Edgar CM, Einhorn TA, Gerstenfeld LC. BMP treatment of C3H10T1/2 mesenchymal stem cells induces both chondrogenesis and osteogenesis. *J Cell Biochem* 2003;90:1112–1127. [PubMed: 14635186]
23. Oh CD, Chun JS. Signaling mechanisms leading to the regulation of differentiation and apoptosis of articular chondrocytes by insulin-like growth factor-1. *J Biol Chem* 2003;278:36563–36571. [PubMed: 12853454]
24. Fukumoto T, Sperling JW, Sanyal A, Fitzsimmons JS, Reinholz GG, Conover CA, O'Driscoll SW. Combined effects of insulin-like growth factor-1 and transforming growth factor-beta1 on periosteal mesenchymal cells during chondrogenesis in vitro. *Osteoarthritis Cartilage* 2003;11:55–64. [PubMed: 12505488]
25. Meinel L, Hofmann S, Betz O, Fajardo R, Merkle HP, Langer R, Evans CH, Vunjak-Novakovic G, Kaplan DL. Osteogenesis by human mesenchymal stem cells cultured on silk biomaterials: comparison of adenovirus mediated gene transfer and protein delivery of BMP-2. *Biomaterials* 2006;27:4993–5002. [PubMed: 16765437]
26. Meinel L, Zoidis E, Zapf J, Hassa P, Hottiger MO, Auer JA, Schneider R, Gander B, Luginbuehl V, Bettschart-Wolfisberger R, Illi OE, Merkle HP, von Rechenberg B. Localized insulin-like growth factor I delivery to enhance new bone formation. *Bone* 2003;33:660–672. [PubMed: 14555272]
27. Raiche AT, Puleo DA. Cell responses to BMP-2 and IGF-I released with different time-dependent profiles. *J Biomed Mater Res A* 2004;69:342–350. [PubMed: 15058007]

28. Woo BH, Fink BF, Page R, Schrier JA, Jo YW, Jiang G, DeLuca M, Vasconez HC, DeLuca PP. Enhancement of bone growth by sustained delivery of recombinant human bone morphogenetic protein-2 in a polymeric matrix. *Pharm Res* 2001;18:1747–1753. [PubMed: 11785696]
29. Palmer GD, Steinert A, Pascher A, Gouze E, Gouze JN, Betz O, Johnstone B, Evans CH, Ghivizzani SC. Gene-induced chondrogenesis of primary mesenchymal stem cells in vitro. *Mol Ther* 2005;12:219–228. [PubMed: 16043093]
30. Kawamura K, Chu CR, Sobajima S, Robbins PD, Fu FH, Izzo NJ, Niyibizi C. Adenoviral-mediated transfer of TGF-beta1 but not IGF-I induces chondrogenic differentiation of human mesenchymal stem cells in pellet cultures. *Exp Hematol* 2005;33:865–872. [PubMed: 16038778]
31. Sriamornsak P. Preliminary investigation of some polysaccharides as a carrier for cell entrapment. *Eur J Pharm Biopharm* 1998;46:233–236. [PubMed: 9795072]
32. Draget KI, Skjak-Braek G, Smidsrod O. Alginate based new materials. *Int J Biol Macromol* 1997;21:47–55. [PubMed: 9283015]
33. Coviello T, Matricardi P, Marianecci C, Alhaique F. Polysaccharide hydrogels for modified release formulations. *J Control Release* 2007;119:5–24. [PubMed: 17382422]
34. Altman GH, Diaz F, Jakuba C, Calabro T, Horan RL, Chen J, Lu H, Richmond J, Kaplan DL. Silk-based biomaterials. *Biomaterials* 2003;24:401–416. [PubMed: 12423595]
35. Kim UJ, Park J, Li C, Jin HJ, Valluzzi R, Kaplan DL. Structure and properties of silk hydrogels. *Biomacromolecules* 2004;5:786–792. [PubMed: 15132662]
36. Jin HJ, Park J, Valluzzi R, Cebe P, Kaplan DL. Biomaterial films of Bombyx mori silk fibroin with poly(ethylene oxide). *Biomacromolecules* 2004;5:711–717. [PubMed: 15132651]
37. Kim UJ, Park J, Kim HJ, Wada M, Kaplan DL. Three-dimensional aqueous-derived biomaterial scaffolds from silk fibroin. *Biomaterials* 2005;26:2775–2785. [PubMed: 15585282]
38. Nazarov R, Jin HJ, Kaplan DL. Porous 3-D scaffolds from regenerated silk fibroin. *Biomacromolecules* 2004;5:718–726. [PubMed: 15132652]
39. Jin HJ, Fridrikh SV, Rutledge GC, Kaplan DL. Electrospinning Bombyx mori silk with poly(ethylene oxide). *Biomacromolecules* 2002;3:1233–1239. [PubMed: 12425660]
40. Wang X, Kludge J, Leisk G, Kaplan DL. Sonication control of silk gelation for cell delivery systems. *Biomaterials* 2008;29:1054–1064. [PubMed: 18031805]
41. Isobe M, Yamazaki Y, Oida SI, Ishihara K, Nakabayashi N, Amagasa T. Bone morphogenetic protein encapsulated with a biodegradable and biocompatible polymer. *J Biomed Mater Res* 1996;32:433–438. [PubMed: 8897149]
42. Oldham JB, Lu L, Zhu X, Porter BD, Hefferan TE, Larson DR, Currier BL, Mikos AG, Yaszemski MJ. Biological activity of rhBMP-2 released from PLGA microspheres. *J Biomech Eng* 2000;122:289–292. [PubMed: 10923299]
43. Kempen DHR, Lu L, Hefferan TE, Creemers LB, Maran A, Classic KL, Dhert WJA, Yaszemski MJ. Retention of in vitro and in vivo BMP-2 bioactivities in sustained delivery vehicles for bone tissue engineering. *Biomaterials* 2008;29:3245–3252. [PubMed: 18472153]
44. Wang X, Wenk E, Matsumoto A, Meinel L, Li C, Kaplan DL. Silk microspheres for encapsulation and controlled release. *J Control Release* 2007;117:360–370. [PubMed: 17218036]
45. Sofia S, McCarthy MB, Gronowicz G, Kaplan DL. Functionalized silk-based biomaterials for bone formation. *J Biomed Mater Res* 2001;54:139–148. [PubMed: 11077413]
46. Meinel L, Illi OE, Zapf J, Malfanti M, Merkle HP, Gander B. Stabilizing insulin-like growth factor-I in poly(D,L-lactide-co-glycolide) microspheres. *J Control Release* 2001;70:193–202. [PubMed: 11166419]
47. Wang Y, Kim UJ, Blasioli DJ, Kim HJ, Kaplan DL. In vitro cartilage tissue engineering with 3D porous aqueous-derived silk scaffolds and mesenchymal stem cells. *Biomaterials* 2005;26:7082–7094. [PubMed: 15985292]
48. Duggirala SS, Mehta RC, DeLuca PP. Interaction of recombinant human bone morphogenetic protein-2 with poly(D,L-lactide-co-glycolide) microspheres. *Pharm Dev Technol* 1996;1:11–19. [PubMed: 9552326]
49. Hannouche D, Terai H, Fuchs JR, Terada S, Zand S, Nasser BA, Petite H, Sedel L, Vacanti JP. Engineering of Implantable Cartilaginous Structures from Bone Marrow-Derived Mesenchymal Stem Cells. *Tissue Eng* 2007;13:87–99. [PubMed: 17518583]

50. Bosnakovski D, Mizuno M, Kim G, Takagi S, Okumura M, Fujinaga T. Chondrogenic differentiation of bovine bone marrow mesenchymal stem cells (MSCs) in different hydrogels: influence of collagen type II extracellular matrix on MSC chondrogenesis. *Biotechnol Bioeng* 2006;93:1152–1163. [PubMed: 16470881]
51. Meinel L, Fajardo R, Hofmann S, Langer R, Chen J, Snyder B, Vunjak-Novakovic G, Kaplan D. Silk implants for the healing of critical size bone defects. *Bone* 2005;37:688–698. [PubMed: 16140599]
52. Karageorgiou V, Tomkins M, Fajardo R, Meinel L, Snyder B, Wade K, Chen J, Vunjak-Novakovic G, Kaplan DL. Porous silk fibroin 3-D scaffolds for delivery of bone morphogenetic protein-2 in vitro and in vivo. *J Biomed Mater Res A* 2006;78:324–334. [PubMed: 16637042]
53. Yuksel E, Weinfeld AB, Cleek R, Waugh J, Jensen J, Boutros S, Shenaq S, Spira M. De Novo adipose tissue generation through long-term, local delivery of insulin and insulin-like growth factor-1 by PLGA/PEG microspheres in an in vivo rat model: a novel concept and capability. *Plst Reconstr Surg* 2000;105:1721 – 1729.
54. Raiche AT, Puleo DA. In vitro effects of combined and sequential delivery of two bone growth factors. *Biomaterials* 2004;25:677–685. [PubMed: 14607506]

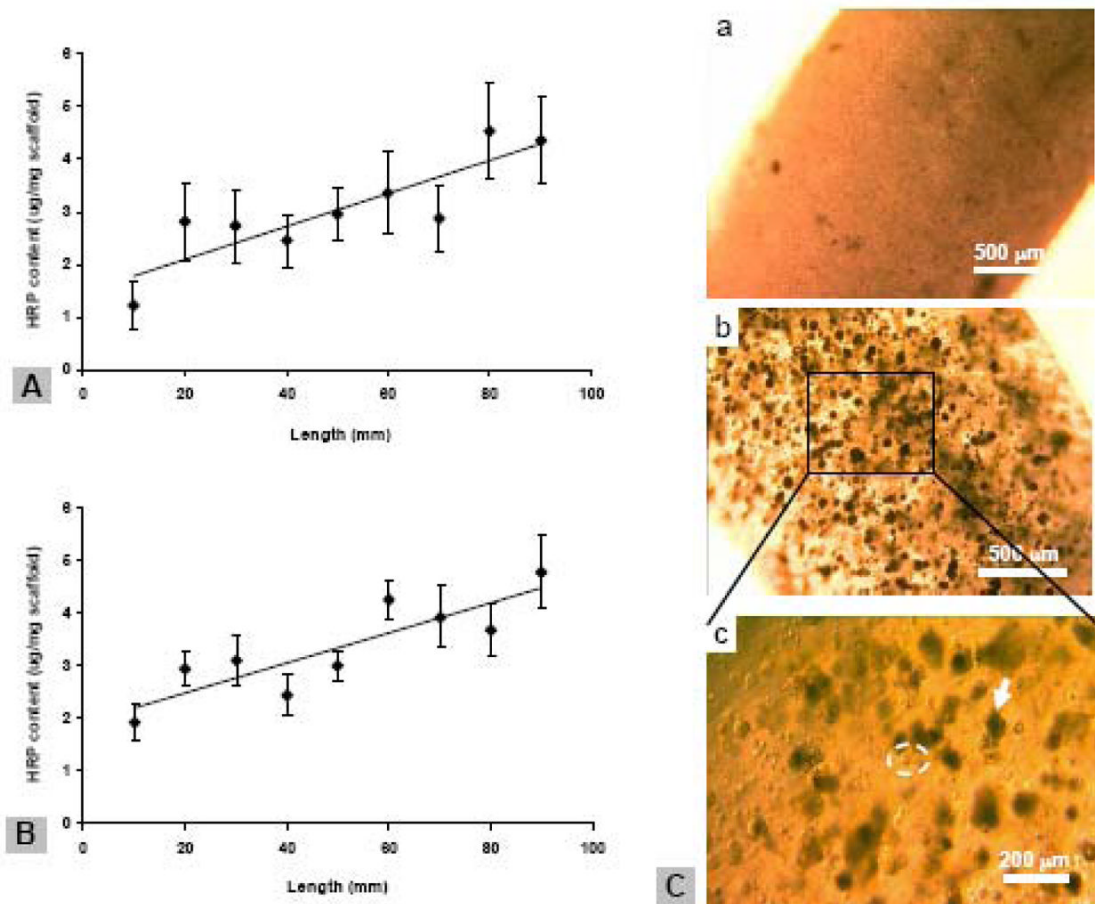
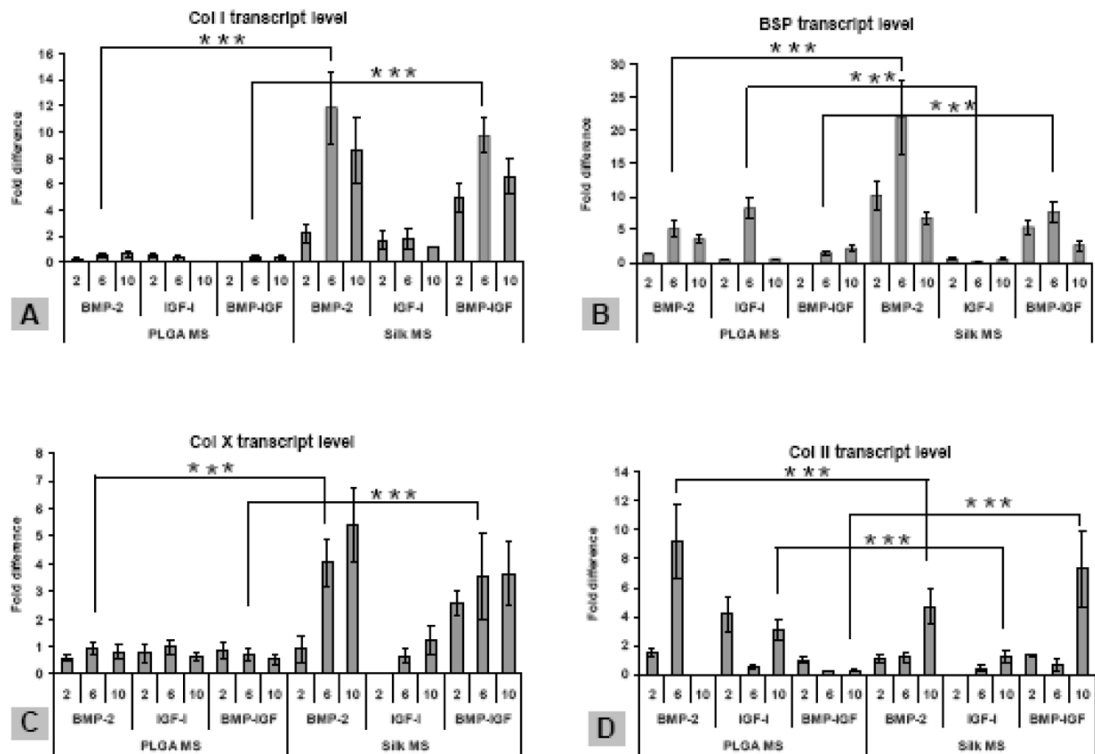


Figure 1.

Characterization of alginate gel scaffolds. **A,B**, gradient distribution of alginate and silk microspheres in alginate scaffolds, respectively, as determined by measuring encapsulated HRP activities. The scaffolds were cut into 9 segments after preparation, and each gel segment was dissolved in 20 mM EDTA and HRP content in the released microspheres was determined. Data represent the Ave.± SD (n = 3). Data were fit linear with least-squares linear regression, $R^2 = 0.75$ for both A and B. **C**, photomicrographs of alginate gel scaffold incorporated with silk (a) and PLGA microspheres (b,c) as well as hMSCs. The scaffolds were cultured in a growth medium for three days before imaging. Arrows indicate PLGA microspheres and circles indicate round shaped hMSCs. Bar = 500 μm in a; 200 μm in b.

**Figure 2.**

Transcript levels from hMSCs in alginate gel scaffolds after 3 weeks culture. For all three groups of scaffolds (rhBMP-2, IGF-I, rhBMP-2/IGF-I), one scaffold was sectioned into 11 segments along the direction of growth factor gradient and analyzed. For the dual growth factor scaffold, rhBMP-2 concentration increased from segment 1 to 11, while the rhIGF-I concentration decreased. The results from segment 2, 6, 10 are presented. **A, B**, Bone makers, collagen type I (Col I) and bone sialoprotein (BSP), respectively. **C**, hypertrophic chondrocyte maker, collagen type X (Col X). **D**, Chondrocyte maker, collagen type II (Col II). *** Extremely significant differences between groups ($P < 0.001$). Data represent the Ave. ± SD ($n = 3-4$)

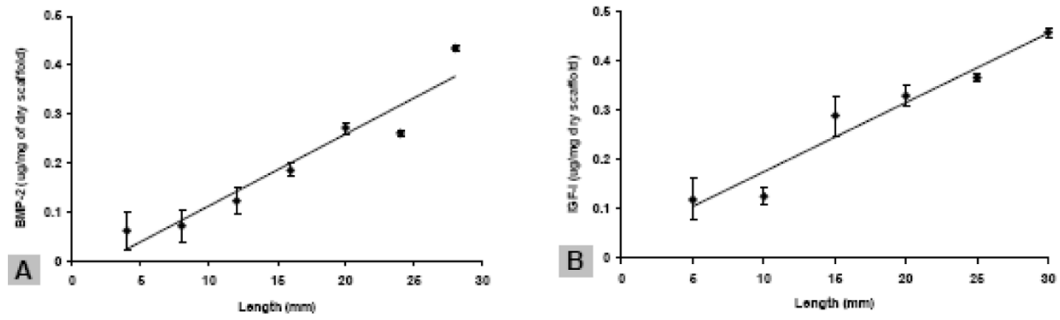


Figure 3. Growth factor gradient in silk microspheres. The scaffold was sectioned into segments and the rhBMP-2 and rhIGF-I content in each segment was quantified by ELISA. Data were fit with least-squares linear regression, $R^2 = 0.92$ and 0.97 for A and B, respectively. **A**, rhBMP-2 gradient. **B**, IGF-I gradient. Data represent the Ave. \pm SD ($n = 3-4$)

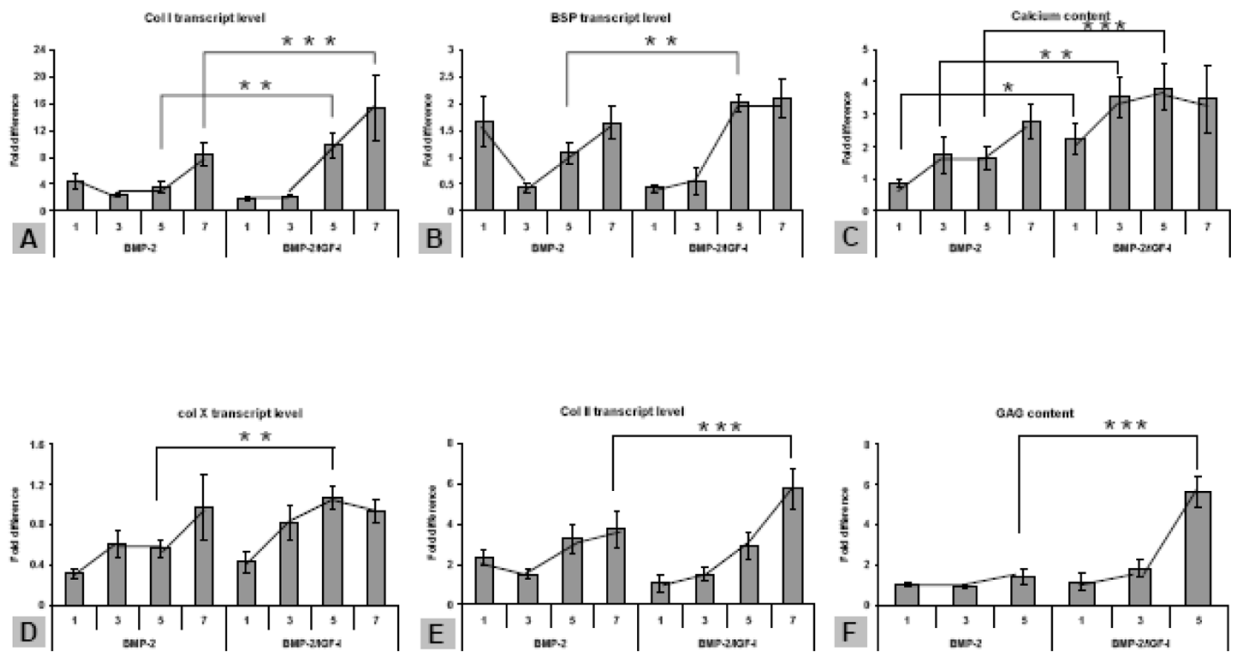


Figure 4.

hMSC osteochondral differentiation in growth factor-gradient silk scaffolds. For all three groups of scaffolds (rhBMP-2, IGF-I, rhBMP-2/IGF-I), scaffolds were sectioned into 7 segments along the direction of growth factor gradient. The results from segment 1, 3, 5, 7 of rhBMP-2 and rhBMP-2/rhIGF-I-incorporated scaffolds are presented. For the scaffolds containing two growth factors, rhBMP-2 concentration increased from segment 1 to 7, while the rhIGF-I concentration decreased. **A, B**, Bone makers, collagen type I (Col I) and bone sialoprotein (BSP), respectively. **C**, calcium deposition as weight percentage per (wet) scaffold segment. **D**, hypertrophic chondrocyte maker, collagen type X (Col X). **E**, Chondrocyte maker, collagen type II (Col II). **F**, formation of cartilage specific extracellular matrix material GAG in a scaffold as weight percentage. *Significant differences between the groups ($P < 0.05$). **Very significant differences between the groups ($P < 0.01$). ***Extremely significant differences between groups ($P < 0.001$). Data are Ave. \pm SD ($n = 3-4$).

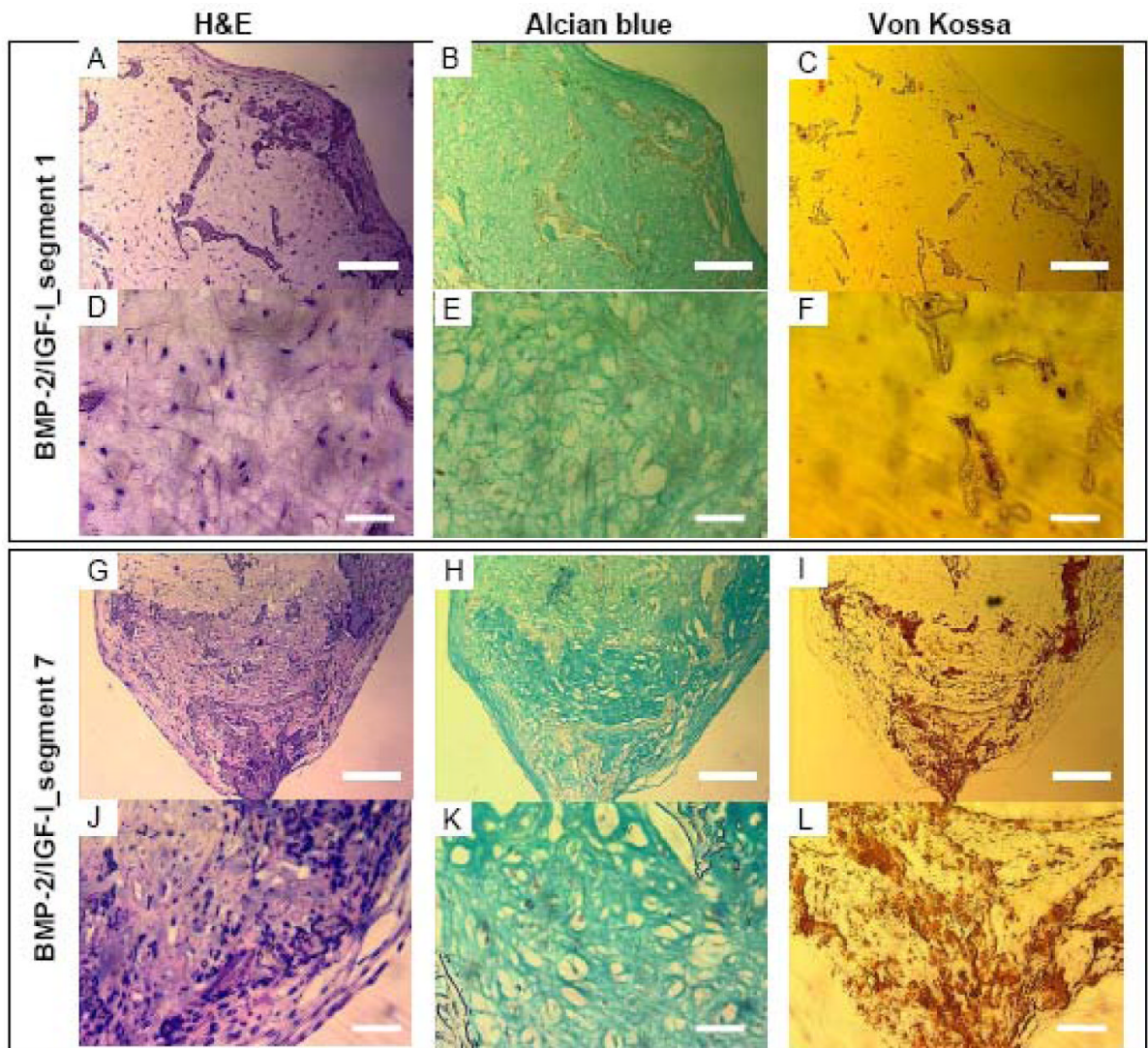


Figure 5. Histological analysis on silk scaffolds with rhBMP-2/rhIGF-I reverse gradient. **A–F**, the first scaffold segment (lowest rhBMP-2 and highest rhIGF-I). **G–L**, the seventh scaffold segment (highest rhBMP-2 and lowest rhIGF-I). **A,D,G,J**, Hematoxylin and eosin (H&E) staining. **B,E,H,K**, Alcian blue staining for proteoglycan formation. **C,F,I,L**, Von Kossa staining for calcium deposition. Scale bars = 200 μm (A–C, G–I) or 50 μm (D–F, J–L)